Figure S1

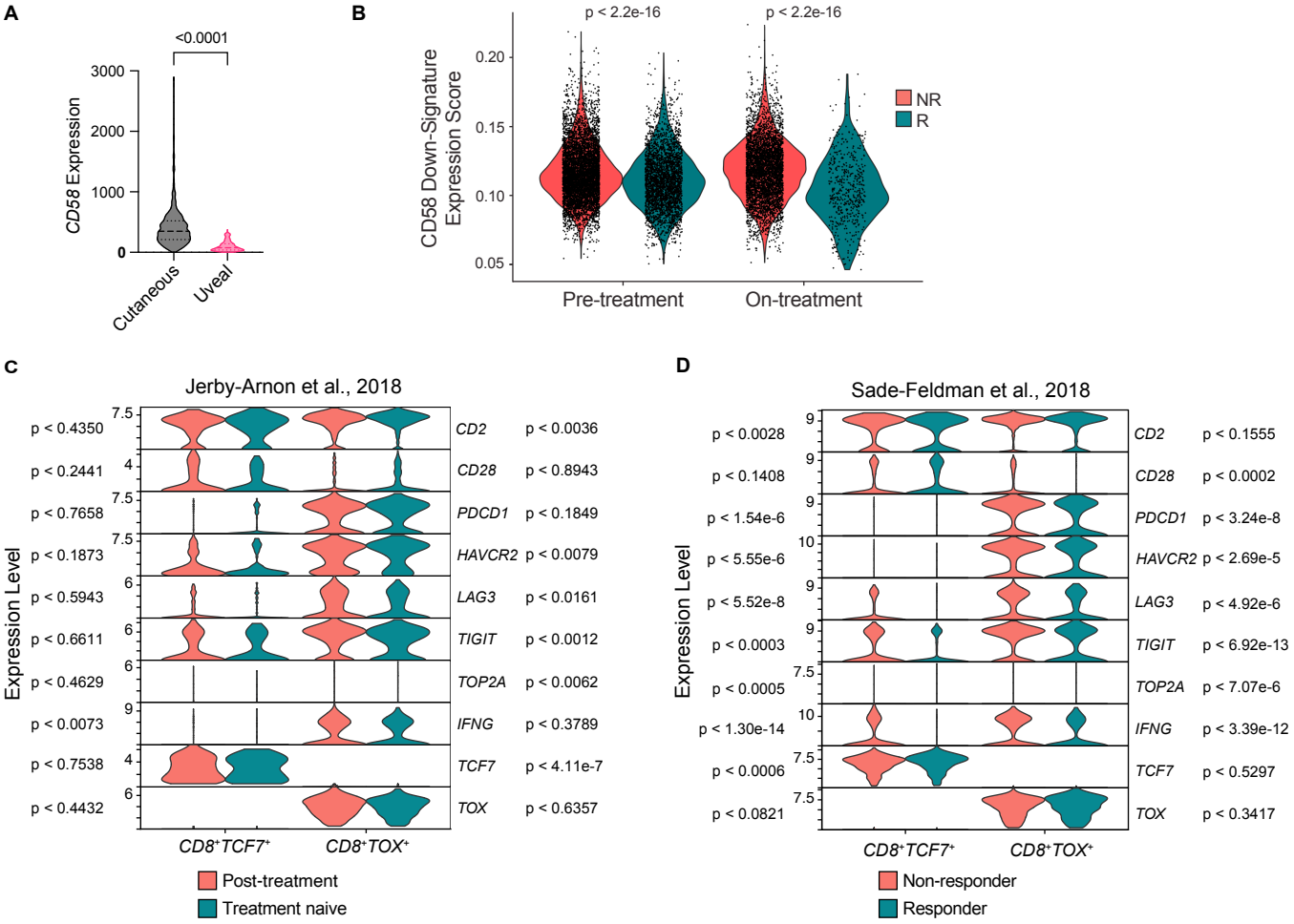
A
<0.0001
CD58 Expression
3000
2000
1000
0
Cutaneous
Uveal
B
p < 2.2e-16
p < 2.2e-16
CD58 Down-Signature Expression Score
0.20
0.15
0.10
0.05
NR
R
Pre-treatment
On-treatment
C
Jerby-Arnon et al., 2018
Expression Level
p < 0.4350
p < 0.2441
p < 0.7658
p < 0.1873
p < 0.5943
p < 0.6611
p < 0.4629
p < 0.0073
p < 0.7538
p < 0.4432
CD2 p < 0.0036
CD28 p < 0.8943
PDCD1 p < 0.1849
HAVCR2 p < 0.0079
LAG3 p < 0.0161
TIGIT p < 0.0012
TOP2A p < 0.0062
IFNG p < 0.3789
TCF7 p < 4.11e-7
TOX p < 0.6357
CD8+TCF7+
CD8+TOX+
Post-treatment
Treatment naive
D
Sade-Feldman et al., 2018
Expression Level
p < 0.0028
p < 0.1408
p < 1.54e-6
p < 5.55e-6
p < 5.52e-8
p < 0.0003
p < 0.0005
p < 1.30e-14
p < 0.0006
p < 0.0821
CD2 p < 0.1555
CD28 p < 0.0002
PDCD1 p < 3.24e-8
HAVCR2 p < 2.69e-5
LAG3 p < 4.92e-6
TIGIT p < 6.92e-13
TOP2A p < 7.07e-6
IFNG p < 3.39e-12
TCF7 p < 0.5297
TOX p < 0.3417
CD8+TCF7+
CD8+TOX+
Non-responder
Responder

Figure S1. **RNA-seq analysis of melanoma patient tumors, Related to Figure 1**

(A) Comparison of *CD58* expression (normalized count shown) in cutaneous and uveal melanomas from TCGA Pan-Cancer Atlas RNASeqV2 data, computed by RSEM. Dotted lines indicate 1st and 3rd quartiles, and dashed lines indicate median.

(B) CD58 down-signature expression scores for malignant cells identified in scRNA-seq analysis of patient melanoma pre- and on-ICB-treatment biopsies from responders versus non-responders shown in Fig. 1A.

(C) scRNA-seq expression data from a previously published dataset of 33 human melanoma tumors from 31 patients[7] split into *CD8*$^+$*TCF7*$^+$ and *CD8*$^+$*TOX*$^+$ T cells. Samples are also separated by treatment status into either treatment-naïve tumors (n=15) or post-ICB resistant tumors (n=15).

(D) As in (C), but analysis is performed on another previously published scRNA-seq dataset of 48 tumor biopsies of metastatic melanoma patients treated with anti-PD-1 therapy[20]. Samples are separated into *CD8*$^+$*TCF7*$^+$ and *CD8*$^+$*TOX*$^+$ T cells, and non-responders (n=31) and responders (n=17).

Statistical analysis performed using Wilcoxon rank sum tests.

Figure S2

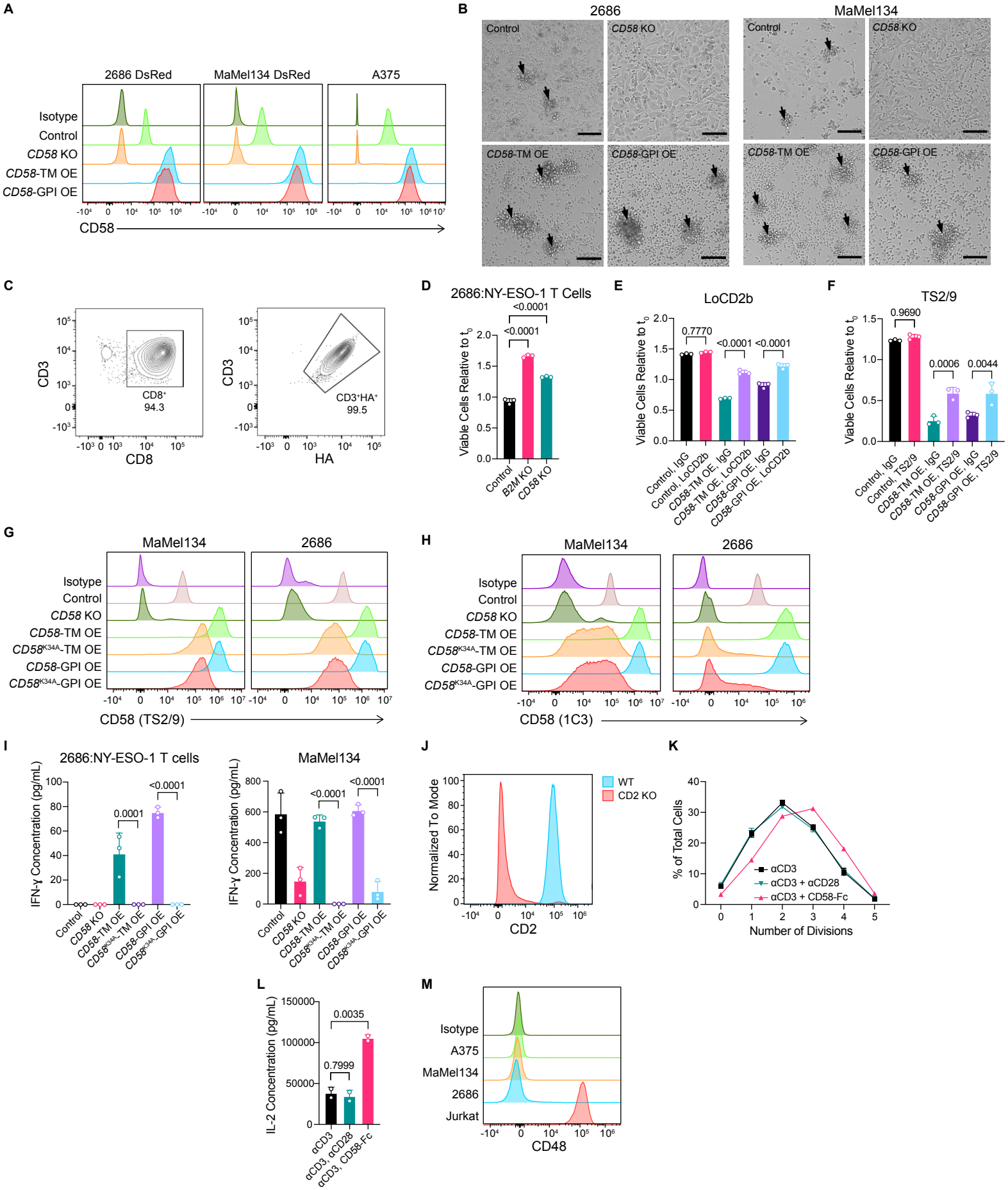
A
2686 DsRed
MaMel134 DsRed
A375
Isotype
Control
CD58 KO
CD58-TM OE
CD58-GPI OE
CD58
B
2686
MaMel134
Control
CD58 KO
CD58-TM OE
CD58-GPI OE
C
CD3
CD8
CD8+
94.3
HA
CD3+HA+
99.5
D
2686:NY-ESO-1 T Cells
Viable Cells Relative to t0
<0.0001
<0.0001
Control
B2M KO
CD58 KO
E
LoCD2b
0.7770
<0.0001
<0.0001
Control, IgG
Control, LoCD2b
CD58-TM OE, IgG
CD58-TM OE, LoCD2b
CD58-GPI OE, IgG
CD58-GPI OE, LoCD2b
F
TS2/9
0.9690
0.0006
0.0044
Control, IgG
Control, TS2/9
CD58-TM OE, IgG
CD58-TM OE, TS2/9
CD58-GPI OE, IgG
CD58-GPI OE, TS2/9
G
MaMel134
2686
Isotype
Control
CD58 KO
CD58-TM OE
CD58K34A-TM OE
CD58-GPI OE
CD58K34A-GPI OE
CD58 (TS2/9)
H
MaMel134
2686
CD58 (1C3)
I
2686:NY-ESO-1 T cells
MaMel134
IFN-γ Concentration (pg/mL)
0.0001
<0.0001
<0.0001
<0.0001
Control
CD58 KO
CD58-TM OE
CD58K34A-TM OE
CD58-GPI OE
CD58K34A-GPI OE
J
Normalized To Mode
WT
CD2 KO
CD2
K
% of Total Cells
αCD3
αCD3 + αCD28
αCD3 + CD58-Fc
Number of Divisions
L
IL-2 Concentration (pg/mL)
0.0035
0.7999
αCD3
αCD3, αCD28
αCD3, CD58-Fc
M
Isotype
A375
MaMel134
2686
Jurkat
CD48

Figure S2. **CD58-CD2 ligation is critical to T-cell-mediated killing across cell lines, Related to Figure 1**

(A) Surface CD58 expression in 2686 DsRed, MaMel134 DsRed, and A375 control, *CD58* KO, and *CD58*-TM or *CD58*-GPI OE cells used in co-culture and flow cytometry experiments.

(B) Widefield images of 2686 and MaMel134 melanoma/TIL co-cultures shown in Figure 1C. Arrowheads indicate T cell clusters following T cell activation. Scale bar = 100 μm.

(C) PBMC-derived T cells were sorted for $CD8^+$ T cells, which were then engineered to express an NY-ESO-1-specific TCR carrying an HA tag. CD8 and HA expression on engineered T cells was assessed by flow cytometry.

(D) Fold change in number of viable cells after 24 h co-culture of 2686 DsRed control, *B2M* KO, and *CD58* KO cells with NY-ESO-1-specific TCR engineered T cells.

(E-F) Fold change in number of viable MaMel134 cells after 48 h co-culture with autologous TILs in the presence of anti-CD2 blocking antibody (LoCD2b) (E), anti-CD58 (TS2/9) blocking antibody (F), or IgG isotype control.

(G-H) Binding of anti-CD58 antibody clones TS2/9 (G) and 1C3 (H) to cell surface CD58 in MaMel134 and 2686 control, *CD58* KO, *CD58*-TM, $CD58^{K34A}$-TM, *CD58*-GPI, or $CD58^{K34A}$-GPI OE cells as assessed by flow cytometry. Clones TS2/9 and 1C3 are known to inhibit CD58-CD2 binding[22,68]. Counts normalized to mode.

(I) IFN-ɣ concentrations in cleared co-culture media from experiments shown in Figure 1E.

(J) Surface CD2 expression of WT and *CD2* KO MaMel134 TILs used in experiment shown in Figure 1F. Counts normalized to mode.

(K-L) MaMel134 TILs were stained with CFSE and stimulated for four days with 1 μg/mL anti-CD3 (OKT3) antibody ± 1 μg/mL anti-CD28 or CD58-Fc chimera. Number of cell divisions was quantified by flow cytometry analysis of remaining CFSE staining (K), and IL-2 concentrations within cleared culture media were quantified by ELISA (L).

(M) Surface CD48 expression in A375, MaMel134, 2686, and positive control Jurkat cells. Counts normalized to mode.

Representative images shown in (B) from at least two independent experiments each. Experiments performed in duplicate (K-L) or triplicate (D-F,I), with representative experiment shown from at least two independent experiments each. Statistical analysis performed using one-way ANOVA with Tukey's multiple comparisons testing. Data represent mean ± SD.

Figure S3

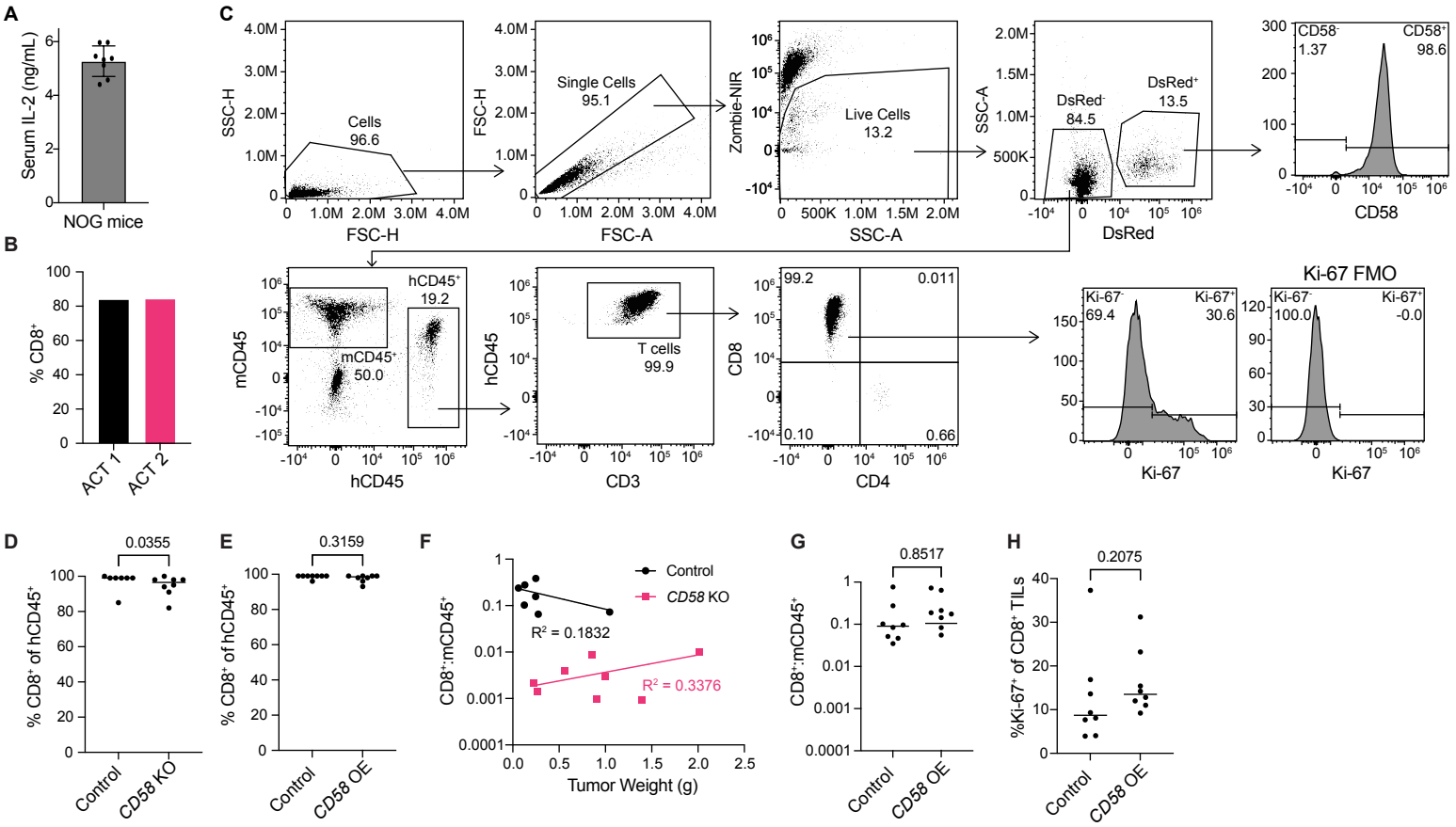
A
Serum IL-2 (ng/mL)
NOG mice
B
% CD8+
ACT 1
ACT 2
C
SSC-H
FSC-H
Cells
96.6
FSC-H
FSC-A
Single Cells
95.1
Zombie-NIR
SSC-A
Live Cells
13.2
SSC-A
DsRed
DsRed-
84.5
DsRed+
13.5
CD58
CD58-
1.37
CD58+
98.6
mCD45
hCD45
hCD45+
19.2
mCD45+
50.0
hCD45
CD3
T cells
99.9
CD8
CD4
99.2
0.011
0.10
0.66
Ki-67 FMO
Ki-67
Ki-67-
69.4
Ki-67+
30.6
Ki-67-
100.0
Ki-67+
-0.0
D
% CD8+ of hCD45+
0.0355
Control
CD58 KO
E
% CD8+ of hCD45+
0.3159
Control
CD58 OE
F
CD8+:mCD45+
Control
CD58 KO
R2 = 0.1832
R2 = 0.3376
Tumor Weight (g)
G
CD8+:mCD45+
0.8517
Control
CD58 OE
H
%Ki-67+ of CD8+ TILs
0.2075
Control
CD58 OE

Figure S3. *CD58* re-expression rescues CD8$^+$ T cell infiltration and effector function within tumors in an *in vivo* model of ACT-treated melanoma, Related to Figure 2

Data shown refer to experiments shown in Fig. 2A.

(A) Example IL-2 serum concentration in NOG mice (n=8).

(B) Percent of CD8$^+$ cells among MaMel134 TILs used for each round of ACT prior to injection.

(C) Flow gating scheme used to identify and phenotype CD8$^+$ human T cells from processed mouse tumors. Fluorescence minus one (FMO) control was used to determine Ki-67 expression.

(D-E) Percent of CD8$^+$ cells among human CD45$^+$ cells within control v. *CD58* KO melanoma tumors (D) and control v. *CD58* OE tumors (E) at experiment endpoint.

(F) Human CD8$^+$:mouse CD45$^+$ ratio within ACT-treated control and *CD58* KO tumors plotted against final tumor weight. Best fit semi-log line shown.

(G-H) Human CD8$^+$:mouse CD45$^+$ ratio (G) and percent of human CD8$^+$ TILs that are Ki-67$^+$ (H) within ACT-treated control and *CD58* OE MaMel134 tumors.

Statistical analysis performed using paired two-sided T-tests. Line at median (D,E,G,H). Data represent mean ± SD (A).

Figure S4

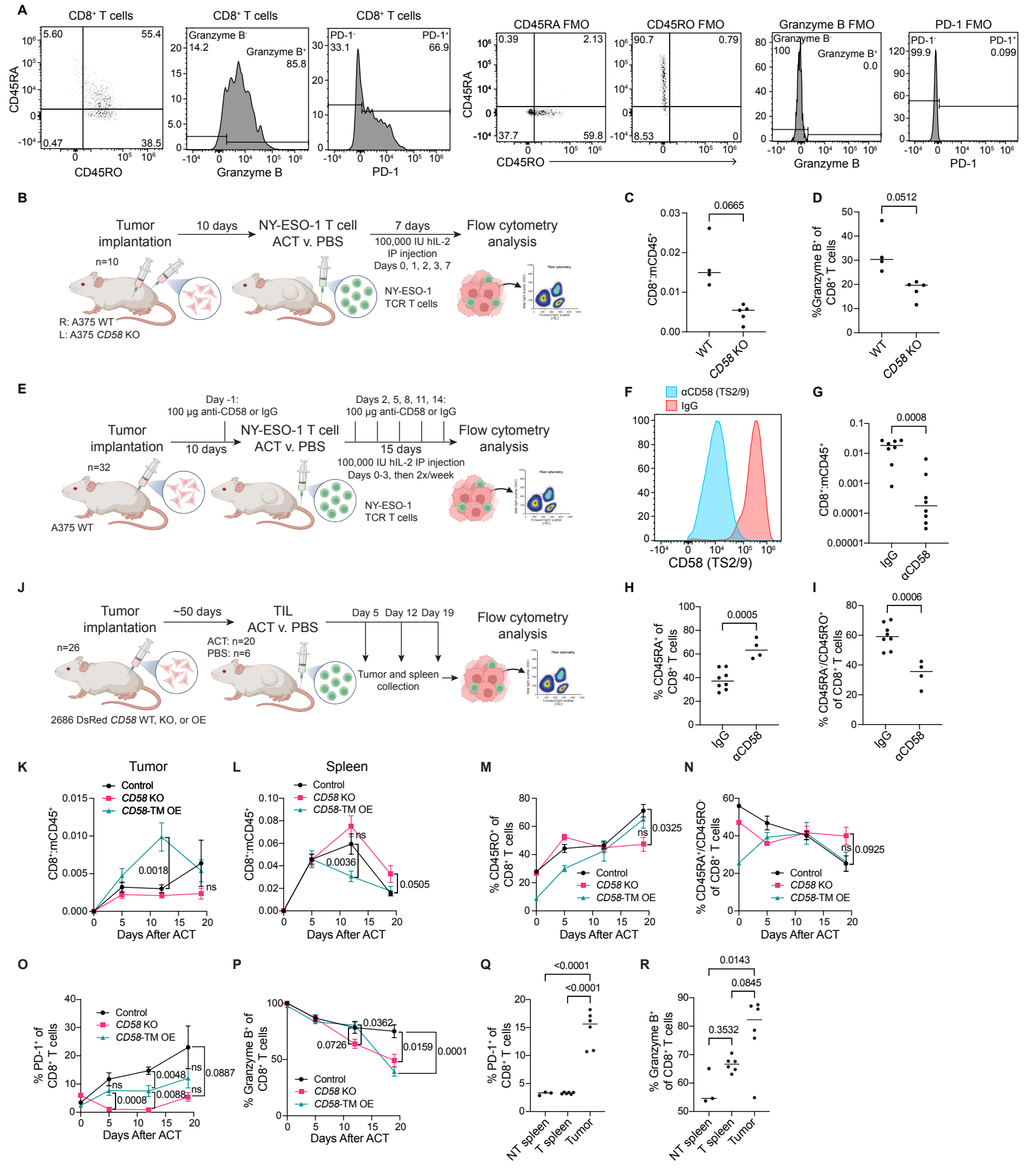
A
CD8⁺ T cells
CD45RA
CD45RO
5.60
55.4
0.47
38.5
Granzyme B
14.2
85.8
PD-1
33.1
66.9
CD45RA FMO
0.39
2.13
37.7
59.8
CD45RO FMO
90.7
0.79
8.53
0
Granzyme B FMO
100
0.0
PD-1 FMO
99.9
0.099
B
Tumor implantation
10 days
NY-ESO-1 T cell ACT v. PBS
7 days
100,000 IU hIL-2 IP injection
Days 0, 1, 2, 3, 7
Flow cytometry analysis
n=10
R: A375 WT
L: A375 CD58 KO
NY-ESO-1 TCR T cells
C
CD8⁺mCD45⁺
0.0665
WT
CD58 KO
D
%Granzyme B⁺ of CD8⁺ T cells
0.0512
E
Day -1: 100 µg anti-CD58 or IgG
Days 2, 5, 8, 11, 14: 100 µg anti-CD58 or IgG
15 days
100,000 IU hIL-2 IP injection
Days 0-3, then 2x/week
n=32
A375 WT
F
αCD58 (TS2/9)
IgG
CD58 (TS2/9)
G
0.0008
IgG
αCD58
J
~50 days
TIL ACT v. PBS
Day 5 Day 12 Day 19
ACT: n=20
PBS: n=6
Tumor and spleen collection
n=26
2686 DsRed CD58 WT, KO, or OE
H
% CD45RA⁺ of CD8⁺ T cells
0.0005
I
% CD45RA⁻/CD45RO⁺ of CD8⁺ T cells
0.0006
K
Tumor
Control
CD58 KO
CD58-TM OE
0.0018
ns
Days After ACT
L
Spleen
0.0036
0.0505
M
% CD45RO⁺ of CD8⁺ T cells
0.0325
N
% CD45RA⁺/CD45RO⁻ of CD8⁺ T cells
0.0925
O
% PD-1⁺ of CD8⁺ T cells
0.0048
0.0008
0.0088
0.0887
P
% Granzyme B⁺ of CD8⁺ T cells
0.0362
0.0726
0.0159
0.0001
Q
<0.0001
<0.0001
NT spleen
T spleen
Tumor
R
0.0143
0.0845
0.3532

Figure S4. **Cancer-cell-intrinsic *CD58* loss is required for early intratumoral T cell infiltration, antigen recognition, and effector function in multiple *in vivo* models of ACT-treated melanoma, Related to Figure 2**

(A) Representative flow plots of $CD8^+$ T cell phenotyping for experiments shown in this figure. Gating used to identify human $CD8^+$ T cells is same as in Figure S3C. FMO controls were used to identify CD45RA-, CD45RO-, PD-1-, and granzyme-B-expressing cells.

(B) NSG mice (n=10) were implanted with A375 WT and *CD58* KO bilateral flank tumors and treated with ACT of NY-ESO-1 TCR-expressing T cells or PBS control (n=5 each) alongside human IL-2 IP injections for T cell maintenance. Tumors were collected 7 days after ACT for analysis by flow cytometry.

(C-D) Human $CD8^+$:mouse $CD45^+$ ratio (C) and percent of human $CD8^+$ T cells that are granzyme B^+ (D) in WT and *CD58* KO ACT-treated tumors from experiment shown in (B).

(E) NSG mice (n=32) were implanted with single A375 WT flank tumors and treated with ACT of NY-ESO-1 TCR-expressing T cells or PBS control (n=16 each), alongside human IL-2 IP injections for T cell maintenance, as well as anti-CD58 (TS2/9) or IgG isotype control (n=8 per group) by IP injection. 15 days after ACT, tumors were collected for analysis by flow cytometry.

(F) Representative plot showing binding of anti-CD58 (TS2/9) PE-Cy5 to cell surface CD58 in non-immune cells (human CD45-/mouse CD45-) of tumors from mice shown in (E) treated with anti-CD58 (TS2/9) blocking antibody or IgG control.

(G-I) Human $CD8^+$:mouse $CD45^+$ ratio (G) or percent of $CD8^+$ T cells that are $CD45RA^+$ (H) or $CD45RA^-/CD45RO^+$ (I) in IgG v. anti-CD58-treated mice from experiment shown in (E).

(J) 2686 *CD58* WT, KO, or TM-OE patient-derived melanoma cells were implanted as single subcutaneous flank tumors (n=26 each), followed by ACT of NY-ESO-1 TCR-expressing T cells (n=20 each) or PBS control (n=6 each). Tumors and spleen were collected at days 5 (n=6 each), 12 (n=6 each), and 19 (n=8 each) after ACT for analysis by flow cytometry.

(K-L) Human $CD8^+$:mouse $CD45^+$ ratio in tumors (K) and spleens (L) of mice shown in (J) days 5, 12, and 19 after ACT.

(M-P) Percentage of $CD8^+$ human T cells within tumors from mice shown in (J) that are $CD45RO^+$ (M), $CD45RA^+/CD45RO^-$ (N), PD-1^+ (O), or granzyme B^+ (P).

(Q-R) Additional NSG mice (n=3) without tumor xenografts were treated as in (J), with spleens collected on day 12 after ACT. Percentage of $CD8^+$ human T cells shown within spleens and tumor from non-tumor-bearing (NT) and *CD58* WT tumor-bearing (T) mice collected at day 12 that are PD-1^+ (Q) or granzyme B^+ (R).

Statistical analysis performed using paired (C-D) and unpaired (G-I) two-sided T-tests or one-way ANOVA with Tukey’s multiple comparisons test (K-R). Line at median. Data represent mean ± SEM (K-P).

Figure S5

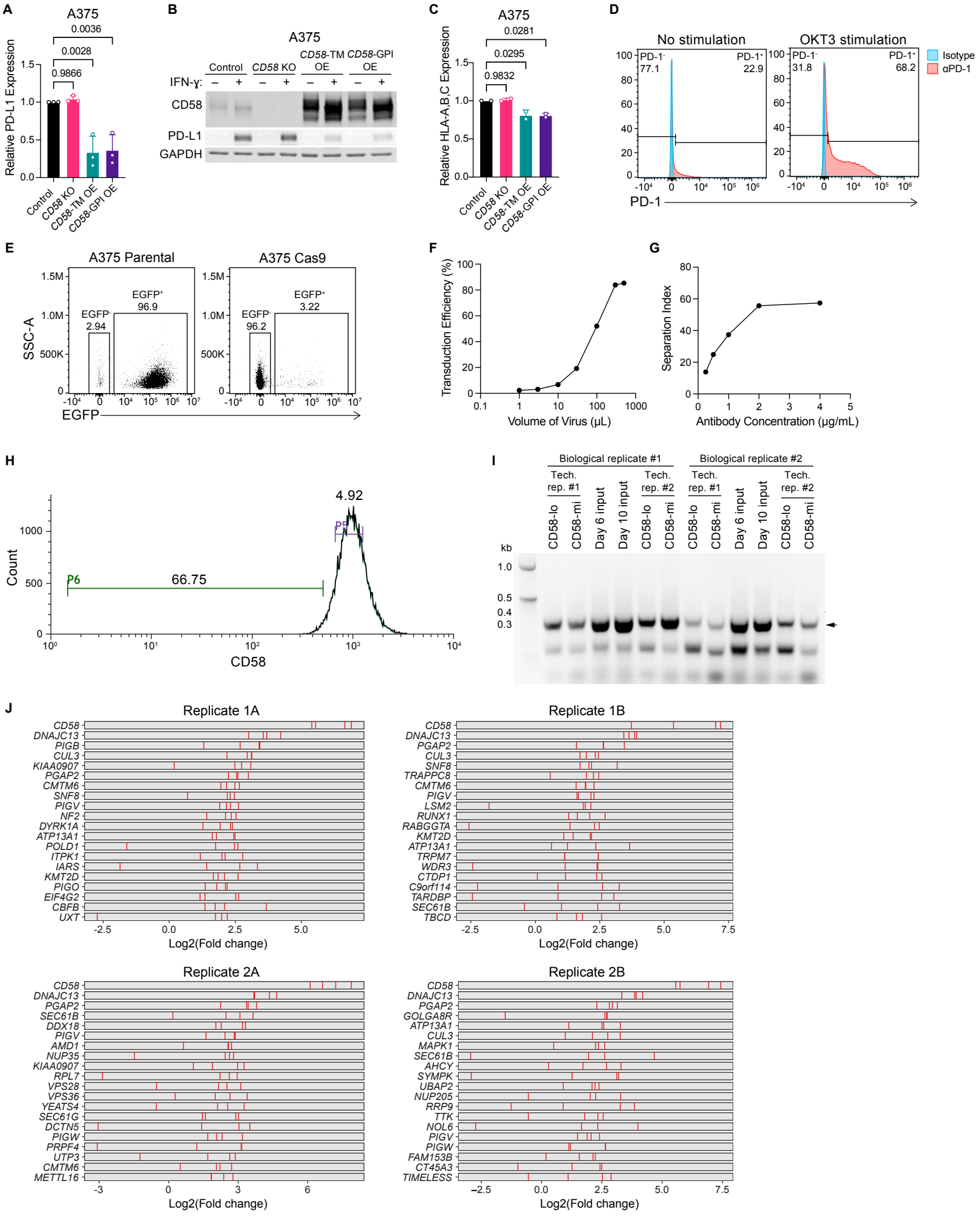
A
A375
0.0036
0.0028
0.9866
Relative PD-L1 Expression
Control
CD58 KO
CD58-TM OE
CD58-GPI OE
B
A375
CD58-TM OE
CD58-GPI OE
Control
CD58 KO
IFN-γ:
CD58
PD-L1
GAPDH
C
A375
0.0281
0.0295
0.9832
Relative HLA-A,B,C Expression
D
No stimulation
OKT3 stimulation
PD-1-
77.1
PD-1+
22.9
31.8
68.2
Isotype
αPD-1
PD-1
E
A375 Parental
A375 Cas9
EGFP+
96.9
EGFP-
2.94
3.22
96.2
SSC-A
EGFP
F
Transduction Efficiency (%)
Volume of Virus (μL)
G
Separation Index
Antibody Concentration (μg/mL)
H
4.92
P6
66.75
Count
CD58
I
Biological replicate #1
Biological replicate #2
Tech. rep. #1
Tech. rep. #2
CD58-lo
CD58-mi
Day 6 input
Day 10 input
kb
1.0
0.5
0.4
0.3
J
Replicate 1A
CD58
DNAJC13
PIGB
CUL3
KIAA0907
PGAP2
CMTM6
SNF8
PIGV
NF2
DYRK1A
ATP13A1
POLD1
ITPK1
IARS
KMT2D
PIGO
EIF4G2
CBFB
UXT
Log2(Fold change)
Replicate 1B
DNAJC13
PGAP2
CUL3
SNF8
TRAPPC8
CMTM6
PIGV
LSM2
RUNX1
RABGGTA
KMT2D
ATP13A1
TRPM7
WDR3
CTDP1
C9orf114
TARDBP
SEC61B
TBCD
Replicate 2A
DNAJC13
PGAP2
SEC61B
DDX18
PIGV
AMD1
NUP35
KIAA0907
RPL7
VPS28
VPS36
YEATS4
SEC61G
DCTN5
PIGW
PRPF4
UTP3
CMTM6
METTL16
Replicate 2B
DNAJC13
PGAP2
GOLGA8R
ATP13A1
CUL3
MAPK1
SEC61B
AHCY
SYMPK
UBAP2
NUP205
RRP9
TTK
NOL6
PIGV
PIGW
FAM153B
CT45A3
TIMELESS

Figure S5. Negative regulation of PD-L1 expression by CD58 and preparation and analysis of CRISPR-Cas9 KO screen to identify regulators of CD58, Related to Figures 3 and 4

(A-B) Surface (A) and whole protein (B) PD-L1 expression in A375 WT, *CD58* KO, *CD58*-TM OE, and *CD58*-GPI OE cells after 72 h with 10 ng/mL IFN-ɣ.

(C) As in (A), but showing HLA-A,B,C expression.

(D) Surface PD-1 expression among $CD8^+$ MaMel134 TILs after overnight stimulation with or without 1 μg/mL anti-CD3 (OKT3) prior to co-culture with autologous melanoma cells shown in Figure 3E. Counts normalized to mode.

(E) Cas9 activity of A375 cells transduced with pLX_311-Cas9 lentivirus was assessed by transduction with pXPR-011 lentivirus encoding both EGFP and EGFP-targeting sgRNA. Percent Cas9 activity represented by percentage of $EGFP^-$ cells.

(F) A375 Cas9-expressing cells were transduced with Brunello genome-wide sgRNA library at increasing virus volumes per 1 million cells for a desired transduction efficiency of 20% (MOI<0.3). 30 μL virus was used for screen.

(G) Anti-CD58-APC antibody was titrated for use in assessing CD58 surface expression in CRISPR-Cas9 screen. 2 μg/mL antibody was used for FACS.

(H) Following 10 days of culturing, CRISPR-Cas9 screen cells were sorted based on CD58 surface expression. Representative gating of $CD58^{lo}$ (P6) and $CD58^{mi}$ (P5) control populations shown.

(I) Following sort of target and control populations, sgRNA sequences were PCR amplified, with a desired PCR product size of ~354 bp (arrow).

(J) Distribution of sgRNA guide enrichment for top 20 gene targets from each replicate of CRISPR-Cas9 screen (Table S2-3). Red bars indicate log2 fold enrichment of each sgRNA per gene within the $CD58^{lo}$ population compared to $CD58^{mi}$ control population for each replicate (biological replicates 1 and 2, each with technical replicates A and B), with genes ranked from top to bottom by increasing P-value.

Experiments performed in duplicate with independent experiments shown (A,C). Representative blot shown of at least two independent experiments (B). Statistical analyses performed using one-way ANOVA with Tukey's multiple comparisons test. Data represent mean ± SD.

Figure S6

A

2686

Gene Name	log(FC) of LFQ intensity	$-\log_{10}(p)$
MAD1L1	6.66	4.62
CMTM6	5.03	3.15
CD58	4.54	2.84
SH2D3C	4.54	2.84

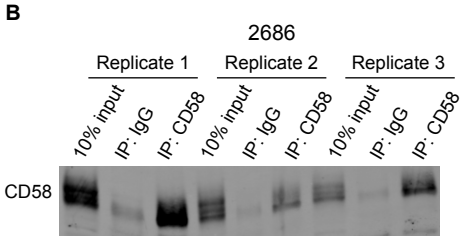

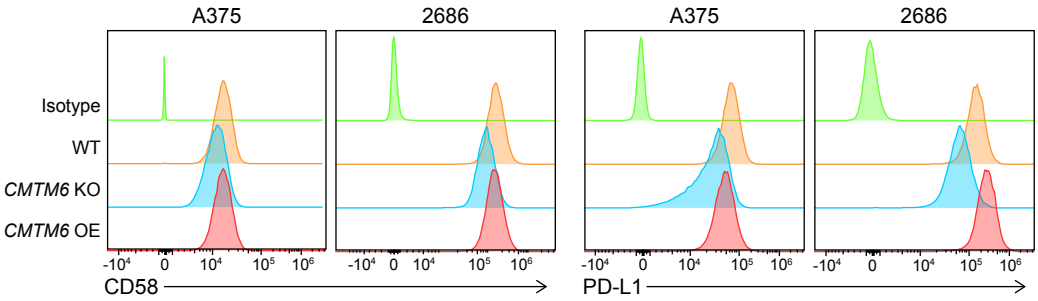

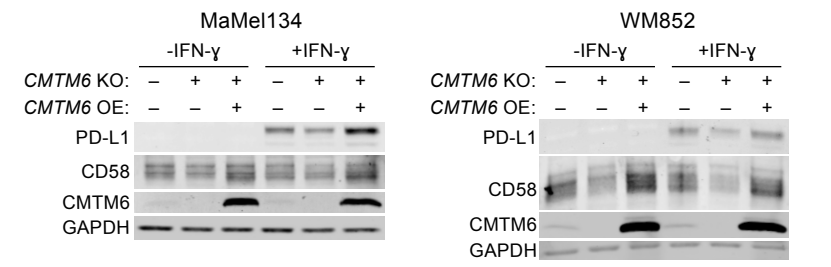

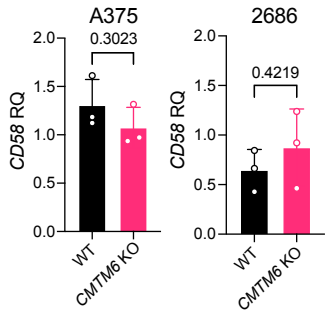

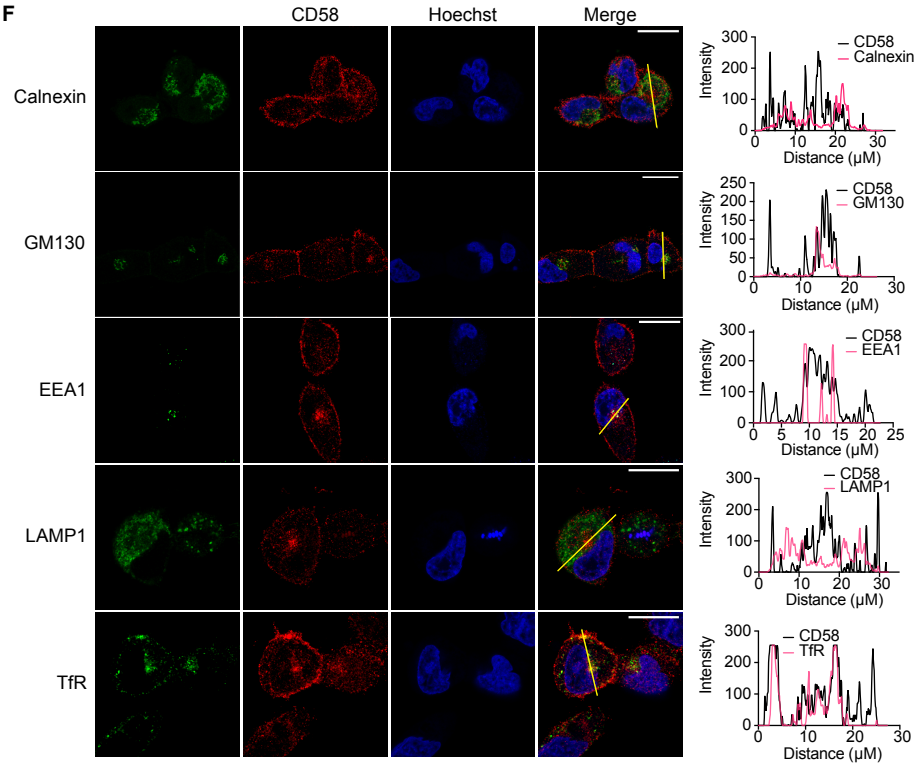

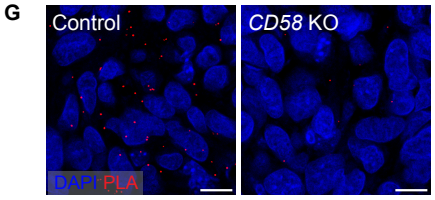

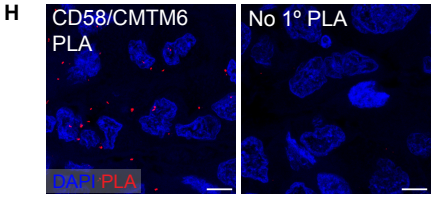

Figure S6. CMTM6 regulates CD58 at a protein level across multiple cell lines, Related to Figure 5

(A) Genes whose encoded proteins were enriched in CD58 IP versus IgG isotype IP lysates from 2686 melanoma cells by mass-spectrometry analysis. Inclusion criteria as in Fig. 5A. Experiment was performed with three biological replicates.

(B) Immunoblotting for CD58 of 2686 CD58 immunoprecipitates used for IP-MS analysis in (A).

(C) Representative flow plots for data shown in Figures 5C-D.

(D) Whole protein PD-L1, CD58, and CMTM6 expression in MaMel134 DsRed and WM852 control, *CMTM6* KO, and *CMTM6* OE cells after 72 h ± 10 ng/mL IFN-ɣ stimulation.

(E) Relative gene expression of *CD58* in A375 and 2686 WT or *CMTM6* KO cells after 72 h with 10 ng/mL IFN-ɣ stimulation.

(F) 2686 WT cells were fixed and immunostained for CD58 alongside markers of ER (Calnexin), Golgi (GM130), early endosomes (EEA1), lysosomes (LAMP1), and recycling endosomes (TfR), and analyzed by confocal microscopy. Profile plots of relative fluorescence intensity along yellow line shown at right. Scale bars = 20 μm.

(G-H) Representative images for data shown in Figure 5I (G) and Figures 5J-K (H). Foci indicating CD58-CMTM6 interactions shown in red. Scale bars = 10 μm.

Representative images shown from at least two independent experiments (D, F). Experiments in (E) each performed with four technical replicates, with independent experiments shown. Statistical analysis performed with two-sided T-test. Data represent mean ± SD.

Figure S7

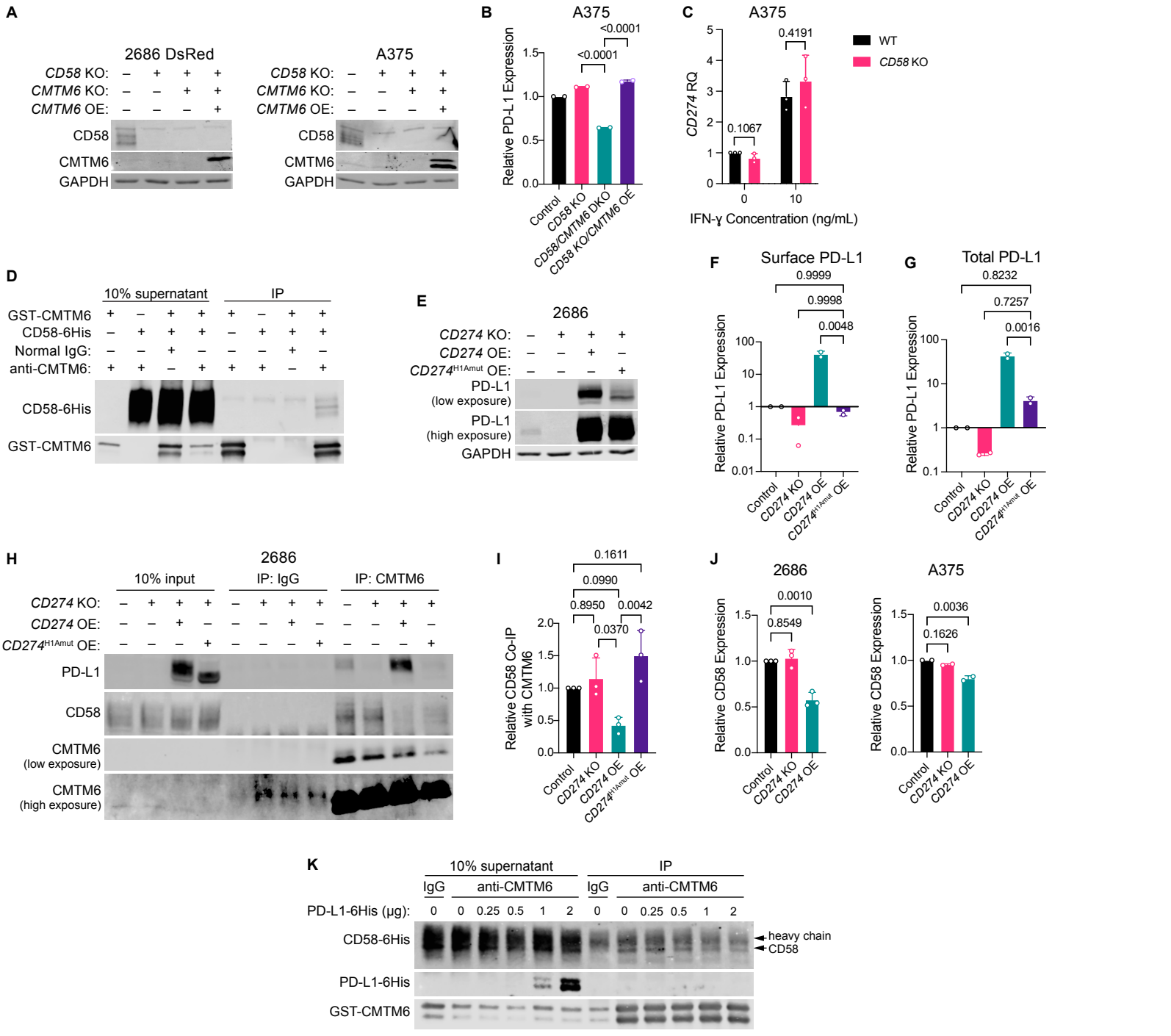
A
2686 DsRed
A375
CD58 KO:
CMTM6 KO:
CMTM6 OE:
CD58
CMTM6
GAPDH
B
A375
Relative PD-L1 Expression
<0.0001
<0.0001
Control
CD58 KO
CD58/CMTM6 DKO
CD58 KO/CMTM6 OE
C
A375
CD274 RQ
0.1067
0.4191
WT
CD58 KO
IFN-γ Concentration (ng/mL)
D
10% supernatant
IP
GST-CMTM6
CD58-6His
Normal IgG:
anti-CMTM6:
E
2686
CD274 KO:
CD274 OE:
CD274H1Amut OE:
PD-L1 (low exposure)
PD-L1 (high exposure)
F
Surface PD-L1
0.9999
0.9998
0.0048
Relative PD-L1 Expression
Control
CD274 KO
CD274 OE
CD274H1Amut OE
G
Total PD-L1
0.8232
0.7257
0.0016
H
2686
10% input
IP: IgG
IP: CMTM6
PD-L1
CD58
CMTM6 (low exposure)
CMTM6 (high exposure)
I
0.1611
0.0990
0.8950
0.0042
0.0370
Relative CD58 Co-IP with CMTM6
J
2686
A375
0.0010
0.8549
0.0036
0.1626
Relative CD58 Expression
K
10% supernatant
IP
IgG
anti-CMTM6
PD-L1-6His (μg):
CD58-6His
PD-L1-6His
GST-CMTM6
heavy chain
CD58

Figure S7. CMTM6 is critical for CD58's regulation of PD-L1, Related to Figure 6

(A) Validation of whole protein CD58 and CMTM6 expression levels of cells used in Figure 6A and S7B.

(B) Surface expression levels of PD-L1 in A375 WT, *CD58* KO, *CD58/CMTM6* DKO, and *CD58* KO/*CMTM6* OE cells after 72 h with 10 ng/mL IFN-ɣ.

(C) Relative gene expression of *CD274* in A375 WT or *CD58* KO cells after 72 h ± 10 ng/mL IFN-ɣ stimulation.

(D) Co-IP of CD58-6His with GST-CMTM6 from a mixture of 5 µg CD58-6His and/or 1 µg GST-CMTM6 purified recombinant proteins.

(E) Immunoblotting for PD-L1 expression in 2686 WT, *CD274* KO, *CD274* OE, and $CD274^{H1Amut}$ OE cells after 72 h with 10 ng/mL IFN-ɣ.

(F-G) Relative surface (F) and total (G) PD-L1 expression in 2686 WT, *CD274* KO, *CD274* OE, and $CD274^{H1Amut}$ OE cells after 72 h with 10 ng/mL IFN-ɣ assessed by surface ± intracellular flow staining of PD-L1.

(H) Co-IP of CD58 and PD-L1 with CMTM6 in 2686 WT, *CD274* KO, *CD274* OE, and $CD274^{H1Amut}$ OE cells after 72 h with 10 ng/mL IFN-ɣ.

(I) Quantification of CD58 co-IP relative to CMTM6 IP shown in (H).

(J) Surface expression levels of CD58 in 2686 and A375 WT, *CD274* KO and *CD274* OE cells after 72 h with 10 ng/mL IFN-ɣ. A375 *CD274* KO cells were not sortable due to lack of baseline PD-L1 expression without IFN-ɣ stimulation; *CD274* KO and OE cells were therefore gated on from mixed population to assess CD58 expression.

(K) Co-IP of PD-L1-6His and CD58-6His protein with GST-CMTM6 protein from a mixture of 1 µg CD58-6His, 1 µg GST-CMTM6, and increasing amounts of PD-L1-6His purified recombinant proteins.

Experiment in (C) performed with four technical replicates, with independent experiments shown. Experiments in (B, F, G, J) performed in duplicate, with independent experiments shown. Independent experiments shown in (I). Representative blots from at least two independent experiments shown (D, E, H, K). Statistical analysis performed using two-sided T-tests (C) and one-way ANOVA with Tukey's multiple comparison testing (B, F, G, I, J). Data represent mean ± SD.

Table S5. P5 and P7 primers for CRISPR-Cas9 KO screen, Related to STAR Methods

OLIGONUCLEOTIDE	SOURCE	IDENTIFIER
P5 0 nt stagger: AATGATACGGCGACCACCGAGATCTACACTCTTTCCCTACACGACG CTCTTCCGATCTTTGTGGAAAGGACGAAACACCG	Doench et al.[26]	N/A
P5 1 nt stagger: AATGATACGGCGACCACCGAGATCTACACTCTTTCCCTACACGACG CTCTTCCGATCTCTTGTGGAAAGGACGAAACACCG	Doench et al.[26]	N/A
P5 2 nt stagger: AATGATACGGCGACCACCGAGATCTACACTCTTTCCCTACACGACG CTCTTCCGATCTGCTTGTGGAAAGGACGAAACACCG	Doench et al.[26]	N/A
P5 3 nt stagger: AATGATACGGCGACCACCGAGATCTACACTCTTTCCCTACACGACG CTCTTCCGATCTAGCTTGTGGAAAGGACGAAACACCG	Doench et al.[26]	N/A
P5 4 nt stagger: AATGATACGGCGACCACCGAGATCTACACTCTTTCCCTACACGACG CTCTTCCGATCTCAACTTGTGGAAAGGACGAAACACCG	Doench et al.[26]	N/A
P5 6 nt stagger: AATGATACGGCGACCACCGAGATCTACACTCTTTCCCTACACGACG CTCTTCCGATCTTGCACCTTGTGGAAAGGACGAAACACCG	Doench et al.[26]	N/A
P5 7 nt stagger: AATGATACGGCGACCACCGAGATCTACACTCTTTCCCTACACGACG CTCTTCCGATCTACGCAACTTGTGGAAAGGACGAAACACCG	Doench et al.[26]	N/A
P5 8 nt stagger: AATGATACGGCGACCACCGAGATCTACACTCTTTCCCTACACGACG CTCTTCCGATCTGAAGACCCTTGTGGAAAGGACGAAACACCG	Doench et al.[26]	N/A
P7 A09: CAAGCAGAAGACGGCATACGAGATCGGTGACCGTGACTGGAGTTCAGACGTG TGCTCTT CCGATCTTCTACTATTCTTTCCCCTGCACTGT	Doench et al.[26]	N/A
P7 A10: CAAGCAGAAGACGGCATACGAGATTACAGAGGGTGACTGGAGTTCAGACGTG TGCTCTT CCGATCTTCTACTATTCTTTCCCCTGCACTGT	Doench et al.[26]	N/A
P7 A11: CAAGCAGAAGACGGCATACGAGATATTGTCAAGTGACTGGAGTTCAGACGTGT GCTCTT CCGATCTTCTACTATTCTTTCCCCTGCACTGT	Doench et al.[26]	N/A
P7 A12: CAAGCAGAAGACGGCATACGAGATTATGTCTTGTGACTGGAGTTCAGACGTGT GCTCTT CCGATCTTCTACTATTCTTTCCCCTGCACTGT	Doench et al.[26]	N/A
P7 B09: CAAGCAGAAGACGGCATACGAGATTAGTTCTTGTGACTGGAGTTCAGACGTGT GCTCTT CCGATCTTCTACTATTCTTTCCCCTGCACTGT	Doench et al.[26]	N/A
P7 B10: CAAGCAGAAGACGGCATACGAGATTACAAGTTGTGACTGGAGTTCAGACGTGT GCTCTT CCGATCTTCTACTATTCTTTCCCCTGCACTGT	Doench et al.[26]	N/A
P7 C09: CAAGCAGAAGACGGCATACGAGATCGTGAGTTGTGACTGGAGTTCAGACGTG TGCTCTT CCGATCTTCTACTATTCTTTCCCCTGCACTGT	Doench et al.[26]	N/A
P7 C10: CAAGCAGAAGACGGCATACGAGATATCAGATTGTGACTGGAGTTCAGACGTGT GCTCTT CCGATCTTCTACTATTCTTTCCCCTGCACTGT	Doench et al.[26]	N/A
P7 C11: CAAGCAGAAGACGGCATACGAGATTAGTGATTGTGACTGGAGTTCAGACGTGT GCTCTT CCGATCTTCTACTATTCTTTCCCCTGCACTGT	Doench et al.[26]	N/A
P7 C12: CAAGCAGAAGACGGCATACGAGATCGGTTCGGGTGACTGGAGTTCAGACGTG TGCTCTT CCGATCTTCTACTATTCTTTCCCCTGCACTGT	Doench et al.[26]	N/A
P7 D09: CAAGCAGAAGACGGCATACGAGATCGCATCTTGTGACTGGAGTTCAGACGTGT GCTCTT CCGATCTTCTACTATTCTTTCCCCTGCACTGT	Doench et al.[26]	N/A

P7 D10: CAAGCAGAAGACGGCATACGAGATATGTTCAAGTGACTGGAGTTCAGACGTGT GCTCTT CCGATCTTCTACTATTCTTTCCCCTGCACTGT	Doench et al.[26]	N/A
P7 G01: CAAGCAGAAGACGGCATACGAGATGCGTAGCCGTGACTGGAGTTCAGACGTG TGCTCTT CCGATCTTCTACTATTCTTTCCCCTGCACTGT	Doench et al.[26]	N/A